First Principles and Semi-empirical Calculations of Atomic and Electronic Structure for the (100) and (110) Perovskite Surfaces

E. Heifets[a], R.I. Eglitis[b], E.A. Kotomin[b,c], and G.Borstel[b]

[a]*Carnegie Institution of Washington, 5251 Broad Branch Rd., N.W. Washington D.C. 20015 and California Institute of Technology, MS 252-21, Pasadena CA 91125*
[b]*Department of Physics, University of Osnabrueck, D-49069 Osnabrueck, Germany*
[c]*Institute for Solid State Physics, University of Latvia, 8 Kengaraga str.,Riga LV-1063, Latvia*

Abstract. We present and discuss results of the calculations for $BaTiO_3$ and $SrTiO_3$ surface relaxation with different terminations using a semi-empirical *shell model* (SM) as well as *ab initio* methods based on Hartree-Fock (HF) and Density Functional Theory (DFT) formalisms. Using the SM, the positions of atoms in 16 near-surface layers placed atop a slab of rigid ions are optimized. This permits us determination of surface rumpling and surface-induced dipole moments (polarization) for different terminations of the (100) and (110) surfaces. We also compare results of the *ab initio* calculations based on both HF with the DFT-type electron correlation corrections, several DFT with different exchange-correlation functionals, and hybrid exchange techniques. Our SM results for the (100) surfaces are in a good agreement with both our *ab initio* calculations and LEED experiments. For the (110) surfaces O-termination is predicted to be the lowest in energy.

INTRODUCTION

Thin films of ABO_3 perovskite ferroelectrics are important for many high tech applications including high capacity memory cells, catalysis, optical waveguides, integrated optics applications, substrates for the high T_c cuprate superconductor growth, etc. [1-4] where surface structure and quality are of primary importance. In this paper, we calculate the atomic structure of the $SrTiO_3$ and $BaTiO_3$ (100) and (110) surfaces for the ideal cubic phases. It should be noted that at all temperatures bulk $SrTiO_3$ exhibits paraelectric properties, despite the antiferrodistortive (AFD) transition at 105 K to a tetragonal phase in which the oxygen octahedra have rotated in opposite directions in neighboring unit cells [5]. In contrast, iso-structural $BaTiO_3$ undergoes several phase transitions from paraelectric to ferroelectric phases as the temperature decreases.

The $SrTiO_3$ (100) surface relaxation has been characterized by means of low energy electron diffraction (LEED), reflection high-energy electron diffraction (RHEED), and medium energy ion scattering (MEIS) measurements [6-10]. Recently, several *ab initio* [11-17] and shell model (SM) [18-20] studies were published for the (100) surface of $BaTiO_3$ and $SrTiO_3$ crystals. Here we perform much more detailed SM

CP582, *Fundamental Physics of Ferroelectrics 2001,* edited by H. Krakauer

studies for both crystals with different terminations, supported by *ab initio* calculations.

The (110) surface only recently became a subject of intensive experimental investigations, focusing mainly on $SrTiO_3$, and using STM, UPS, XPS, Auger spectroscopies, and LEED [21]. Here we report the first simulations of (011) surfaces of $BaTiO_3$ and $SrTiO_3$ crystals. We performed these (110) surface simulations using SM.

METHOD

In the present study we studied a two-dimensional slab of cubic $SrTiO_3$ and $BaTiO_3$ crystals by means of the SM [22] as realized in the MARVIN computer code [23]. To study the surface relaxation, we optimized the atomic positions in several (varied from one to 16) near-surface planes, placed into the electrostatic field of the slab (simulated by 20 additional planes whose atoms were fixed in their perfect lattice sites). The number of these additional planes was chosen to reach a convergence of the crystalline field in the surface planes.

In our slab calculations we simulated Ti- and Sr(Ba)-terminated (100) surfaces as well as Ba-, Ti- and O-terminated (110) surfaces. For each termination surface, modification was characterized by the surface rumpling (*s*), interplane distances between top metal and the second crystal layers (d_{12}), and between the second and the third crystal layer (d_{23}). Our calculations of the interplane distances are based on the metal ion (Ti or Sr) displacements from unrelaxed planes, which are known to be much stronger electron scatterers than O ions [6]. In SM calculations, atoms from one to 16 near-surface planes were allowed to relax in order to achieve the minimum total energy. As a result, we obtain the optimized slab geometry and dipole moments caused by core and electron shell displacements from regular lattice sites. The surface energy was calculated as $E_s=E_{tot}-E_1$ -n E_{bulk}, where E_{tot} is the total energy for a slab of *n* relaxed planes placed on the rigid substrate, E_{bulk} the total energy per bulk unit cell, and E_1 the interaction energy between relaxed slab and rigid substrate.

To check our SM results, we also performed *ab initio* calculations based on HF with different DFT *posteriori* electron correlation corrections to the total energy (including generalized gradient approximation, GGA, Perdew-91, and Lee, Yang, Parr (LYP)) as well as the Kohn-Sham equation with a number of exchange-correlation functionals (LDA, PBE, PWGGA), including *hybrid* HF-DFT exchange functionals (B3LYP, B3PW) [24]. For this purpose we used the CRYSTAL-98 computer code [24] using the Gaussian-type basis set, and we optimized atomic positions in several top layers of $SrTiO_3$ slab consisting of 7 planes terminated by Ti and O atoms on both sides of the slab.

In both SM and ab initio simulations we used a single slab and had no periodicity along z axis. All interactions across the slab were summed directly. Ewald procedure was applied only for summation of Coulomb interactions in two dimensions along the slab. Therefore, our calculations took into account the depolarization field.

MAIN RESULTS

A. The (100) Surfaces

Table 1 gives the displacement magnitudes for atomic cores and shells as found in SM calculations for three top layers nearby the surface. Our calculations show that Ti^{4+}, Sr^{2+}, and O^{2-} ions in the planes close to the surface reveal different displacements from their perfect crystalline sites. One can also see the difference between the SrO- and TiO_2-terminated surfaces. In most cases the surface ions are displaced inwards, whereas the ionic displacements in the second layer point outwards from the crystal. In particular, on the SrO-terminated surface of $SrTiO_3$, the surface ions shift inwards by 7% of the bulk lattice constant (a_0=3.89 Å) whereas in the third layer the displacements of Sr ions are reduced to 1.4 %. Similarly, on the BaO-terminated surface of $BaTiO_3$, the surface ions shift inward by 3.7% of bulk lattice constant (a_0=3.96 Å) and by 0.5% in the third layer. Ti ions in the second layer of the $SrTiO_3$ crystal are displaced outwards by ≈1.6%. In $BaTiO_3$ this value is ≈1.3%. Inward displacement of Ti in the fourth layer in both crystals is ≈ 0.2%. The cores of O ions in the first plane in both crystals are displaced outward, but their shells are displaced inward, which means strong O atom polarization. *Both* O cores and shells in the second (TiO_2) layer relax outwards the crystals.

Very similar trends in ionic displacements are observed for the Ti-terminated surface (Table 1). Inward displacements of the surface Ti ions are ≈ 3% in $SrTiO_3$ (≈ 2.7 % in $BaTiO_3$) and outward displacements of Sr ions in the second layer are nearly the same in magnitude. The O ions are displaced inwards in the top layer; again we can see the opposite displacement directions for the O cores and shells in the second plane.

Table 1. SM relaxation of the uppermost three layers in the Sr- and Ti-terminated (100) $SrTiO_3$ surfaces. Totally 16 near-surface planes were allowed to relax. Ionic displacements are in percents of a_0=3.89Å (the bulk crystal lattice parameter). Positive (negative) displacements mean the direction outwards (inwards) the surface. Numbers in brackets are results of previous *ab initio* plane wave with pseudopotentials calculations[12].

Sr-terminated				Ti-terminated			
Layer	Ion	Type	Δz(%)	Layer	Ion	Type	Δz(%)
1	Sr^{2+}	Core	-7.10(-5.7)	1	Ti^{4+}	core	-2.96(-3.4)
		Shell	-5.03			shell	-2.88
	O^{2-}	Core	1.15 (0.1)		O^{2-}	core	-1.73 (-1.6)
		Shell	-3.15			shell	-2.40
2	Ti^{4+}	Core	1.57 (1.2)	2	Sr^{2+}	core	3.46 (2.5)
		Shell	1.53			shell	2.63
	O^{2-}	Core	0.87 (0.0)		O^{2-}	core	-0.21 (-0.5)
		Shell	1.21			shell	1.34
3	Sr^{2+}	Core	-1.42 (-1.2)	3	Ti^{4+}	core	-0.60 (-0.7)
		Shell	-1.10			shell	-0.59
	O^{2-}	Core	0.70 (-0.1)		O^{2-}	core	-0.29 (-0.5)
		Shell	-0.58			shell	-0.43

Table 2. Relaxation of uppermost three layers (per cent of lattice constant) for Ti-terminated $SrTiO_3$ (100) found in the *ab initio* HF with different electron correlation corrections and DFT calculations (see in the text).

A. Ti-terminated $SrTiO_3$ surface													
N	Ion	[11]	[17]	DFT (Kohn Sham)						Hartree-Fock with *posteriori* corrections			
				LDA	B3LYP	B3PW	BLYP	PBE	PWGGA	HF	HFGGA	HF P91	HFLYP
1	Ti^{4+}	-3.4	-1.79	-2.12	-2.03	-2.19	-2.28	-1.88	-2.31	-2.74	-3.20	-3.19	-3.05
	O^{2-}	-1.6	-0.26	-1.11	-0.72	-0.93	-0.90	-0.57	-1.19	-1.38	-2.20	-2.20	-1.87
2	Sr^{2+}	2.5	4.61	2.21	2.38	2.18	2.64	2.75	2.04	1.91	1.81	1.83	1.87
	O^{2-}	-0.5	0.77	0.07	0.21	0.01	0.12	0.45	0.0	-0.13	-0.15	-0.17	-0.17
3	Ti^{4+}	-0.7	-0.26							-0.26	-0.28	-0.28	-0.28
	O^{2-}	-0.5	0.26							-0.05	-0.13	-0.14	-0.14

B. Sr-terminated $SrTiO_3$ surface													
N	Ion	[11]	[17]	DFT (Kohn Sham)						Hartree-Fock with *posteriori* corrections			
				LDA	B3LYP	B3PW	BLYP	PBE	PWGGA	HF	HFGGA	HF P91	HFLYP
1	Sr^{2+}	-5.7	-6.66	-8.48	-4.28	-4.29	-2.78	-4.25	-4.28	-2.61	-4.16	-4.13	-3.74
	O^{2-}	0.1	1.02	-2.37	0.64	0.61	2.28	1.02	0.90	1.56	0.41	0.35	0.10
2	Ti^{4+}	1.2	1.79	-0.42	1.16	1.25	1.85	1.27	1.29	0.79	0.48	0.48	0.56
	O^{2-}	0.0	0.26	-0.87	0.85	0.82	1.35	0.73	0.61	0.51	0.23	0.17	0.27
3	Sr^{2+}	-1.2	-1.54							-0.49	-0.69	-0.69	-0.70
	O^{2-}	-0.1	0.26							0.01	-0.25	-0.02	-0.14

Along with SM calculations, we performed *ab initio* calculations for the $SrTiO_3$ surfaces, after first testing them for the bulk properties. LDA calculations underestimate the lattice constant a_0 (by 0.8%) and overestimate the bulk modulus B by 4.5 %. The hybrid B3PW method gives a better result for B (Δ=4%) and only by 0.5% *overestimates* a_0. The HF method without any correlation corrections overestimates a_0 only by 1% but considerably overestimates B (by 16%). Lastly, HF with GGA corrections makes a_0 too small (Δ = -1.5%) but B even larger (Δ= 37%). In other words, it is quite difficult to choose the optimal method reproducing all properties equally well, but the hybrid B3PW method looks like the best one.

Atomic displacements in several top $SrTiO_3$ planes calculated using the *ab initio* methods (see Table 2) are in a good agreement with SM results and discussed *ab initio* plane wave calculations [11, 17]. Both DFT and HF with correlation effects predict Sr displacement on the Sr-terminated surface to be larger than that for Ti atom on the Ti-terminated surface, in agreement with previous plane wave calculations [11,17].

Table 3 gives atomic displacements, the effective static charges (obtained with the Mulliken population analysis), and bond populations between nearest metal and oxygen atoms. Let us use B3PW results for the analysis. The main effect observed well here is strengthening of the Ti-O chemical bond near the surface. Its population on the Ti- terminated surface is 124 me, which is about one and a half times larger than the relevant values in the bulk (82 me). The Ti-O populations between the first

and second, the second and third plane, and lastly, the third and fourth planes (124 me, 92 me, and 86 me) also exceed the bulk value. In contrast, the Sr-O populations are very small and even negative which indicates the repulsion. This effect is also well seen from the effective charges: that for Sr is close to the formal ionic charge of 2e, whereas charges for Ti and O atoms are much smaller than the ionic charges of 4e, and -2e, respectively, due to the covalent bonding between them.

Next, we performed SM calculations of the surface energy, E_s, for the relaxed surfaces. Its magnitude saturates when more than 8 near-surface planes are allowed to relax. In the case of Ba-terminated $BaTiO_3$ surface, E_s=1.45 eV/cell, which is only slightly larger then that for the Ti-terminated case (1.40 eV). This tiny difference appears entirely due to the difference in the relaxation energies of the surfaces in both cases. Since the difference is very small, both types of surfaces should co-exist, which is confirmed by both *ab initio* calculations [5] and experiments [6]. For $SrTiO_3$, the Ti-terminated surface energy of 1.37 eV is slightly larger than that for Sr- termination (1.33 eV/cell). The *ab initio* calculations [11, 12] gave quite similar average surface energies (1.26 eV/cell and 1.24 eV/cell for $SrTiO_3$ and $BaTiO_3$, respectively.)

The surface dipole moments for different numbers of relaxed layers oscillate as the number of relaxed near-surface layers increases from one to six. For a larger number

Table 3. Calculated absolute atomic displacements d (in Å), the effective atomic charges Q (in e) and bond populations P between nearest Me-O atoms (in me) for the Ti and Sr-terminations

A. TiO_2-terminated $SrTiO_3$ surface

N	Ion		DFT		Hartree - Fock	
			B3PW	B3LYP	HF	HFGGA
1	Ti^{4+}	d	-0.086	-0.079	-0.107	-0.1245
		Q	2.165	2.197	2.507	2.502
		P	128	124	146	142
	O^{2-}	d	-0.037	-0.028	-0.054	-0.0856
		Q	-1.241	-1.257	-1.395	-1.400
		P	-10	-10	-28	-30
2	Sr^{2+}	d	0.085	0.094	0.074	0.0705
		Q	1.833	1.834	1.890	1.888
		P	-10	-8	-20	-20
	O^{2-}	d	0.0004	0.008	-0.005	-0.006
		Q	-1.297	1.307	-1.418	-1.401
		P	92	92	104	104
3	Ti^{4+}	d			-0.010	-0.011
		Q	2.269	2.313	2.553	2.552
		P	86	86	114	114
	O^{2-}	d			-0.002	-0.005
		Q	-1.363	-1.376	-1.476	-1.476
		P	-10	-8	-22	-22
Bulk	Ti^{4+}	Q	2.272	2.325	2.584	2.50
		P	82	74	112	100
	O^{2-}	Q	-1.375	-1.392	-1.497	-1.466
		P	-10	-8	-20	-28
	Sr^{2+}	Q	1.852	1.852	1.909	1.898

B. SrO-terminated $SrTiO_3$ surface

N	Ion		DFT		Hartree - Fock	
			B3PW	B3LYP	HF	HFGGA
1	Sr^{2+}	d	-0.168	-0.168	-0.102	-0.162
		Q	1.829	1.833	1.897	1.894
		P	-4	-2	-20	-20
	O^{2-}	d	0.024	0.025	0.061	0.016
		Q	-1.44	-1.459	-1.581	-1.555
		P	166	160	198	208
2	Ti^{4+}	d	0.049	0.046	0.031	0.019
		Q	2.24	2.282	2.536	2.524
		P	56	58	90	84
	O^{2-}	d	0.32	0.033	0.020	0.009
		Q	-1.423	-1.434	-1.517	-1.523
		P	-10	-8	-20	-20
3	Sr^{2+}	d			-0.019	-0.027
		Q	1.857	1.855	1.907	1.906
		P	-10	-8	-22	-22
	O^{2-}	d			0.0	-0.01
		Q	-1.398	-1.409	-1.508	-1.503
		P	80	80	108	108
Bulk	Ti^{4+}	Q	2.272	2.325	2.584	2.50
		P	82	74	112	100
	O^{2-}	Q	-1.375	-1.392	-1.497	-1.466
		P	-10	-8	-10	-28
	Sr^{2+}	Q	1.852	1.852	1.909	1.898

of relaxed layers these oscillations practically vanish and the dipole moments saturate at the level of 0.1-0.2 eÅ. Note that the same number of layers (six) was found by us as necessary to reach convergence of the crystalline field in the surface region. For both $SrTiO_3$ surfaces and Ti-terminated $BaTiO_3$ surfaces, the dipole moments are negative, whereas for Ba-termination it turns out to be positive (but close to zero). In all cases, a large polarization of ions in the near-surface layers takes place. It manifests itself through the large difference in displacements of cores and shells of the same ions.

A comparison of our SM calculations for the surface structure with the *ab initio* plane-wave studies [11,12],other SM simulations[19] and experimental results [6,7,9] is presented in Table 4. The agreement of our results with the plane-wave ab initio calculations and the experimental data is very good. We observe also only qualitative agreement with other SM calculations for $SrTiO_3$ [18-20] (Table 4). Anyway, all theoretical methods give the same signs for both the rumpling and change of the interplanar distances.

The results of the LEED and RHEED experiments [6-8] presented in the same Table 4 suggest relaxations quite different from calculated quantities. Note also that the results of these two experiments contradict each other (e.g., in the sign of the d_{12} for Sr- terminated surface). Both our simulations and calculations [11] gave values, which are closer to the experimental data [6]. Lastly, it was found in recent MEIS experiments [9] for the Ti-terminated $SrTiO_3$ surface that $s \approx 2$ %, which is close to our result in Table 4.

However, despite a good agreement for the O and Ti atom displacements from the top plane relative to each other, one serious question remains open: both experiments argue that the topmost O atoms move outwards from the surface, whereas all calculations give that in most cases O goes inwards the surface.

B. The (110) Surfaces

The problem with calculating the (110) surfaces of SrTiO3 and $BaTiO_3$ is that they consist of charged planes. If the (110) surface was to be modeled exactly as one would expect after crystal cleavage, it would have an infinite dipole moment perpendicular to the surface which makes the surface unstable. To avoid this problem, in our calculations we removed half of O atoms from the O-terminated surface, the Sr (Ba) atoms from the Ti-terminated surface, and Ti and O atoms from the Sr (Ba)-terminated surface [22] (Fig.1). As a result, we obtain the so-called *type-II* stable surface with charged planes but a zero dipole moment [25]. The initial atomic configuration for the O-terminated surface, where every second surface O atom is removed and others occupy the same sites as in the bulk structure (Fig.1b), we call hereafter *asymmetric* denoted in oncoming Tables as *A*. Since such a removal of half of O atoms disturbs the balance of interatomic forces along the surface, we studied also another, *symmetric* initial surface configuration (denoted as *B*) in which the O atom is placed in the *middle* of the distance between two equivalent O atoms in the bulk (Fig.1a,c).

Table 4 Surface rumpling *s*, and relative displacements of the three near-surface planes for the Sr(Ba)- and Ti-terminated $SrTiO_3$ and $BaTiO_3$ (100) surfaces (in percents of the bulk lattice parameters).

	$SrTiO_3$					
	Sr-terminated			Ti-terminated		
Method	*s*	d_{12}	d_{23}	*s*	d_{12}	D_{23}
Present study (SM)	8.2	-8.6	3.0	1.2	-6.4	4.0
Shell model [19]	4.5	-4.75	1.45	1.1	-3.95	1.2
Ab initio [11]	5.8	-6.9	2.4	1.8	-7.0	3.2
LEED experiment [6]	4.1±2	-5±1	2±1	2.1±2	1±1	-1±1
RHEED experiment [7,8]	4.1	2.6	1.3	2.6	1.8	1.3
	$BaTiO_3$					
	Ba-terminated			Ti-terminated		
Method	*s*	d_{12}	d_{23}	*s*	d_{12}	D_{23}
Present study (SM)	2.7	-5.0	1.8	1.8	-4.9	2.5
Ab initio [12]	1.4	-3.7	1.5	2.3	-5.2	2.0

The calculated surface energies for Ba-, Sr-, Ti-terminations of $BaTiO_3$ and $SrTiO_3$ (Table 5) are much larger than those for the (001) surfaces. The O-terminated asymmetric surfaces have considerably lower energies for both $BaTiO_3$ and $SrTiO_3$. These energies turn out to be close to those for the (100) surface. Thus, O-termination should be predominant when crystal is cleaved or grown along the (011) plane. On the other hand, symmetrical O-termination is energetically costly and thus unfavorable.

Table 6 gives the predicted values for surface rumpling and the relative displacements of the two top layers. For the Ti-terminated surface, the rumpling for both $SrTiO_3$ and $BaTiO_3$ (110) surfaces is similar and very large, ≈ 13-14 %. This relaxation is much larger than what we found for the (100) surface. The reduction of relative distances between the first three layers is quite similar for both crystals, being about 4-5 %. Note also that surface ions are strongly polarized.

For the O-terminated surface, when O ions are placed initially into symmetrical (*B*) surface positions, all near-surface atoms are displaced along the *z* axis perpendicular to the surface. On the other hand, if O ions in $SrTiO_3$ and $BaTiO_3$ are placed initially in asymmetrical positions (*A*), atoms reveal also in-plane displacements, i.e., in the direction *parallel* to the surface. As a result, we found another optimized surface structure, with considerably smaller surface energy. In this structure, Ba (Sr) atoms in the second plane are only moderately (≈4 %) shifted outwards. But now the surface O ions tend to move inwards, so that they are displaced along the *z* axis by as much as 11-14 %. The surface O ions are strongly polarized; the relative core-shell separation is ≈ 4 %. As a result, the first and second planes turn out to be compressed. Their separation is reduced by ≈12 %. The distance between the second and third planes increases by ≈9 % because of the strong O atom inward displacements in the third plane. Note that these O atoms are also strongly polarized. Similar to the (100) surface, the (110) surface-induced dipole moments oscillate as the number of relaxed

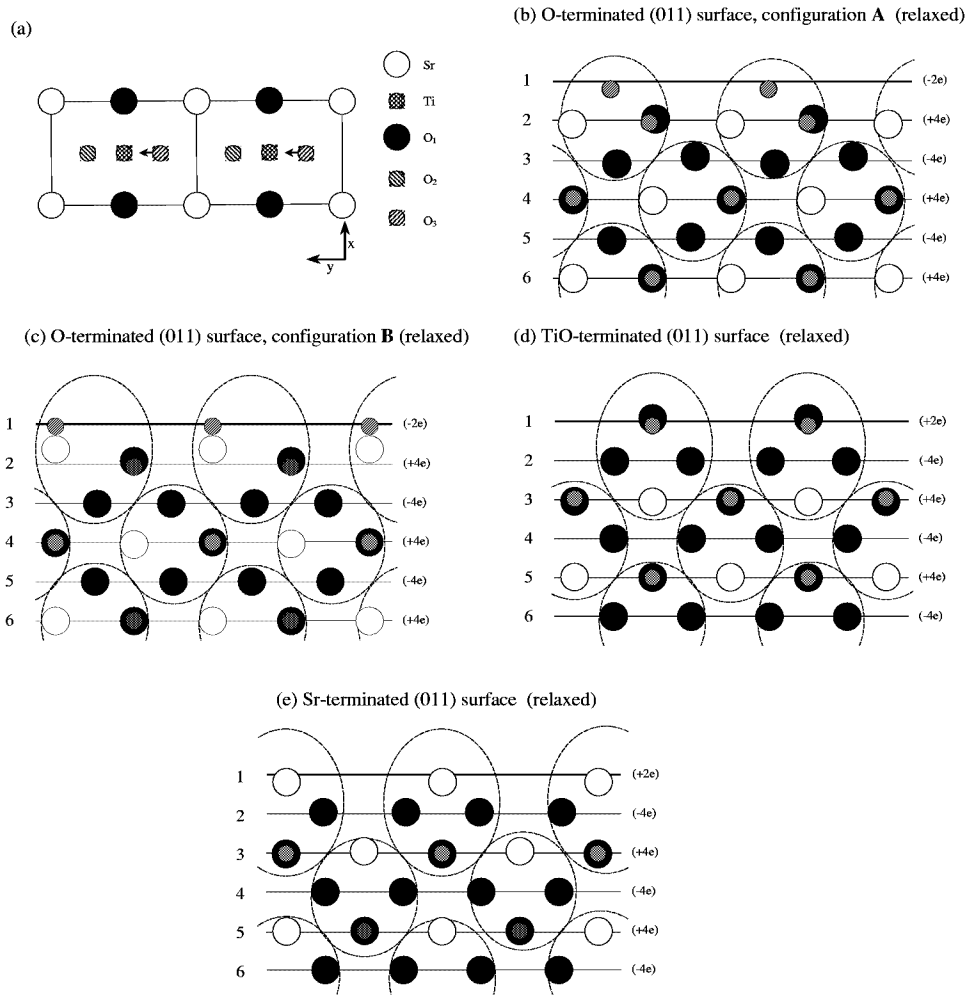

Fig.1. (a) Top view of the (110) O-terminated surface, directions of the O atom displacements are shown by arrows. In our model, we remove atoms O_2 from the O-terminated surface and search for the atomic relaxations when O_3 are placed initially into asymmetric A or symmetric B positions (see text for explanations). Atoms of Ti, Sr, and O_1 lie in the second plane below the O-surface plane. (b,c) Side view of the two possible configurations A and B after relaxation. (d,e) Relaxed TiO- and Sr-terminated surfaces. Dashed ellipses containing 5 atoms in the 3 nearest planes show neutral fragments from which the surface unit cell is built. Numbers in brackets on the right-hand side indicate the corresponding effective charges of related planes in the cell.

Table 5. Surface energies (in eV/unit cell) for (011) $BaTiO_3$ and $SrTiO_3$ surfaces with different terminations calculated by means of SM

Termination	Surface energies	
	$BaTiO_3$	$SrTiO_3$
Ba(Sr)-terminated	4.2	3.4
TiO-terminated	2.3	2.4
O-terminated (A), asymmetric	1.8	1.6
O-terminated (B), symmetric	4.8	3.4

Table 6. Surface rumpling *s*, and relative displacements of the three near-surface plane for the O- and Ti-terminated $SrTiO_3$ and $BaTiO_3$ (110) surfaces (in percents of the bulk lattice parameter) obtained for the symmetrical initial O position **B**. Numbers in brackets correspond to the asymmetrical O position **A**.

	O-terminated		Ti-terminated		
	Δd_{12}	Δd_{23}	*s*	Δd_{12}	Δd_{23}
$SrTiO_3$	2.36(-11.83)	-2.73(8.69)	14.47	-4.27	-3.86
$BaTiO_3$	3.34	-3.89	13.38	-5.27	-3.25

near-surface layers increases from one to ten. Then these oscillations vanish and the dipole moment saturates. The values of the surface dipole moments perpendicular to the $BaTiO_3$(110) saturate at the -0.93 e Å for Ba-terminated and -1.61 e Å for Ti-terminated surfaces.

This is in sharp contrast with the results for the (100) surface for which we got dipole moments of 0.07 e Å in the case of the Ba-termination, and -0.19 e Å for the Ti-terminated surfaces. That is, the (110) surface dipole moments and respectively, surface polarizations, are much larger. In contrast, for the O-terminated $BaTiO_3$ in both initial configurations- asymmetric and symmetric- dipole moments are positive and of the same order of magnitude as for the Ba-, Ti-terminations. It is, however, important to stress, that in the asymmetric O configuration A we observe also the strong on-plane polarization p_y caused by the dipole moments much larger than those perpendicularly to the surface. This is a manifestation of the ferroelectric reconstruction predicted for the first time for the (100) surface [18].

The perpendicular surface polarization of Sr- and Ti-terminated $SrTiO_3$ is quite similar to that for the $BaTiO_3$. However, dipole moments for the O-terminated asymmetric $SrTiO_3$ surface reveal strong oscillations even for 16 relaxed layers (similar to those observed above for the surface energy). This is caused by this surface instability with respect to the AFD-type relaxation, which is observed for $SrTiO_3$ at low temperatures. In contrast, p_y dipole moment for the symmetric O configuration saturates rapidly to zero.

DISCUSSION AND CONCLUSION

A comparison of our semi-empirical SM results with *our ab initio* HF and DFT as well as with previous plane wave pseudopotential calculations [11-13] and experimental low-energy electron diffraction [6] studies of $SrTiO_3$ (001) surface clearly

demonstrates their good agreement for the *rumpling* and the relative displacements of the second and third planes. We found that the metal-terminated surface relaxations for $SrTiO_3$ and $BaTiO_3$ (110) surfaces are much larger than those for the (100) surfaces. This is in a line with observations for other oxides. Another important prediction of our calculations is that the asymmetric O-termination is the energetically most favorable amongst all (110) surface terminations. The formation of large dipole moments parallel and perpendicular to the relaxed surface even in a cubic phase of perovskite could considerably affect the ferroelectric properties of thin ferroelectric films.

ACKNOWLEDGMENTS

This study was partly supported by DAAD (grant to EK through Osnabrück University) and by ONR grant #N00014-97-1-0052 to R. E. Cohen. Authors are indebted to R. E. Cohen, R. Dovesi, C.R.A. Catlow, F. Cora, S. Dorfman, D. Fuks, and D. Vanderbilt for fruitful discussions.

REFERENCES

1. Noguera C, *Physics and Chemistry at Oxide Surfaces*, Cambridge Univ. Press, N.Y., 1996.
2 Lines M.E., and Glass A.M., *Principles and Applications of Ferroelectrics and Related Materials*, Clarendon, Oxford, 1977.
3 Auciello O., Scott J.F., and Ramesh R., *Physics Today*, July 1998, pp.22-30.
4 Proceedings of the Williamsburg workshop on Ferroelectrics-99, *J. Phys. Chem. Sol.*, **61**, No 2 (2000).
5 Zhong W, and Vanderbilt D., *Phys. Rev.* B **53,** 5047-5055 (1996).
6 Bickel N., Schmidt G., Heinz K., and Müller K., *Phys. Rev. Lett.* **62,** 2009-2013 (1989).
7 Hikita T., Hanada T., Kudo M., Kawai M., *Surf. Sci.* **287/288,** 377-380 (1993).
8 Kudo M., Hikita T., Hanada T., Sekine R., and Kawai M., *Surf. and Interf. Analysis*, **22,** 412-416 (1994).
9 Ikeda A., Nishimura T., Morishita T., and Kido Y., *Surf. Sci.* **433-435,** 520-525 (1999).
10 Nishimura T., Ikeda A., Namba H., Morishita T., Kido Y., *Surf. Sci.* **421,** 273-278 (1999).
11 Padilla J., and Vanderbilt D, *Surf. Sci.* **418,** 64-70 (1998).
12 Padilla J., and Vanderbilt D, *Phys. Rev.* B **56,** 1625-1630 (1997).
13 Meyer B., Padilla J., and Vanderbilt D, *Faraday Discussions*, **114,** 395-405 (1999).
14 Cora F., and Catlow C.R.A., *Faraday Discussions*, **114,** 421-430 (1999).
15 Cohen R.E., *Ferroelectrics* **194**, 323-342 (1997).
16 Fu L., Yashenko E., Resca L., and Resta R., *Phys. Rev.* B **60**, 2697-2703 (1999).
17 Cheng C., Kunc K., and Lee M.H., *Phys. Rev.* B, **62**, 10409-10417 (2000).
18 Ravikumar V., Wolf D., and Dravid V.P., *Phys. Rev. Lett.*, **74**, 960-964 (1995).
19 Prade J., Schröder U., Kress W., and de Kulkarni F.W., *J. Phys: Condens. Matter*, **5**, 1-15 (1993).
20 Tinte S., and Stachiotti M.G., *AIP Conf. Proc* **535** ed. R Cohen, 273-282 (2000).
21 H.Bando H., Aiura Y., Haruyama Y., Shimizu T.,and.Nishihara Y., *J. Vac. Sci. Technol.*, B **13,** 1150-1158 (1995); Szot K., and Speier W., *Phys. Rev.* B **60,** 5909-5920 (1999); .Jiang O.D., and Zegenhagen J., *Surf. Sci.* **425,** 343-350 (1999); .Souda R., *Phys. Rev.* B **60,** 6068-6074 (1999).
22 Heifets E., Kotomin E.A., and Maier J., *Surf. Sci.*, **462,** 19-35 (2000).
23 Gay D.H., and Rohl A.L., *J. Chem. Soc. Faraday Trans.* **91,** 925-935 (1995).
24 Saunders V.R., Dovesi R., Roetti C., Causa M., Harrison N.M., Orlando R. and Zicovich-Wilson C.M., *Crystal-98 User Manual* (University of Torino, 1999).
25 Tasker P.W., *J. Phys. C : Solid State Phys.*, **12,** 4977-4986 (1979).